

A New Design for DC-DC Converter Topology with MISO for Renewable Energy Resources

S.Sathishkumar, M.Valan Rajkumar, S.Vinoth Kumar, M.Maruthamuthu, A.Soundar, A.Kumaresann
Department of Electrical and Electronics Engineering, Gnanamani College of Technology, Namakkal-637018, India.

Abstract –A dual DC input power supply for high output efficiency DC-DC converter is developed. The proposed converter can boost the varied voltages of different power supply in the sense of hybrid power supply to obtain a stable output dc voltage for the load demand. Based on the varied situations the operational mode of the proposed converter can be divided into two modes including a single power supply mode and dual power supply mode .In dual power supply state the input circuits are connected in series get added together with the designed pulse width modulation can greatly reduce the conduction loss of the switches. Single mode power supply will operate whenever it is capable to meet the load demand, when it cannot meet the load demand then dual power supply mode will be operate. The proposed high efficiency DC-DC converter with dual input power supply greatly reduces the conduction and switching losses in the system. This topology is developed to cope with the demerits of large size, complex topology, and expensive cost in conventional converter with single power supply mode. MATLAB has been used to make the model and simulate the system and PI controller is used.

Index Terms –DC-DC Converter, hybrid power supply

1. INTRODUCTION

One of the major concern of power generation sector is day to day increasing power demand .Based on the current scenario all over the world especially India has lot of power shortage issues. The power developed from the fossil fuels are becoming so less as it degrade the environment and getting depleted day by day [1-5]. So now days we are looking forward for the power generation from renewable energies like solar, wind, biomass, tidal etc which does not create any pollution to the environment. At present stand-alone solar PV system has been promoted around this global level on comparatively larger scale but this independent system cannot provide continuous energy as they are seasonal hence hybrid systems come into play. As the solar radiation varies throughout the day, the power generated also varies [6-10]. Maximum power point trackers (MPPTs) play an important role because they maximize the power output for a set of conditions, and therefore maximize the efficiency generation from renewable energies like solar, wind, biomass, tidal etc which does not create any pollution to the environment [11-15].

The use of renewable energy is helping the environment to reduce the global warming effect. In rural areas or remote areas

where grid cant supply the power there we can use this proposed dual input power source to meet the load demand.. The input impedance of the DC-DC converter is matched with the optimum impedance of PV panel. This method has good performance under MATLAB [15-20]. Based on the environmental concern and the energy status, the developed electrical power may be insufficient to drive the load. To have the continuous power supply, we use hybrid power supply by using different kinds of sources. Those sources can be capacitor, fuel cell, rechargeable battery or best source renewable energies [20-28].

2. BLOCK DIAGRAM

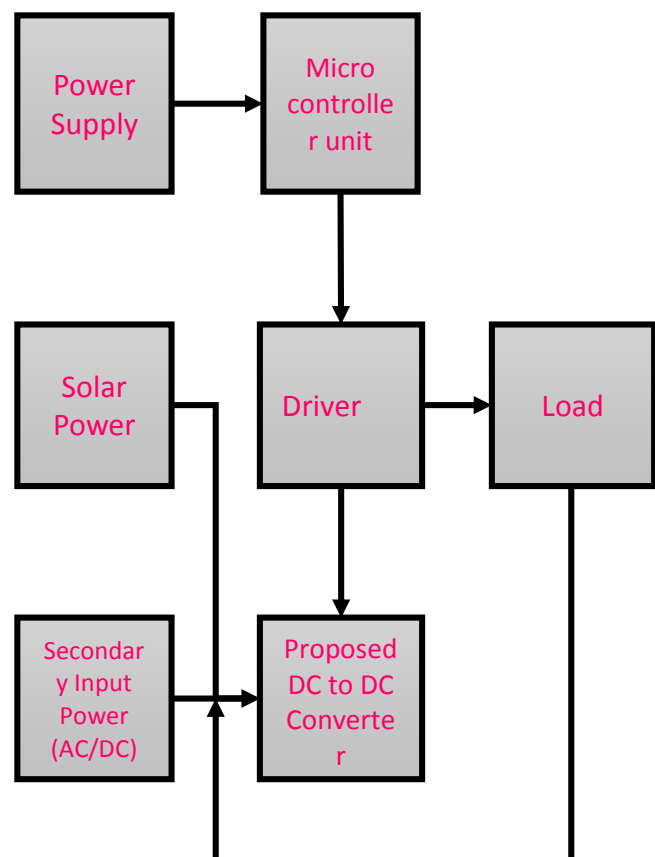


Figure: 1- block diagram.

When the multi inputs are used in DC-DC converter simultaneous power will be delivered from all the sources which is not required at all the time, hence it increases complexity and cost of the system. As well the system design requires enlarged storage equipment independently. This paper helped in studying and modelling the PV panel using PV cell circuit model. Where the PV cell is been derived from the PN junction and it reflects the characteristics of the cell. In this paper we have come to know that how the conduction loss is been reduced across the switch, how the efficiency of the system is improved, Much more than the hard switching converter.

This block diagram shows the way in which the dual input is fed to the boost converter. Solar and AC supply are the two input sources used here, these two sources are fed together to a boost converter to power the load based on load demand, so that the load demand is satisfied continuously.

Hence to know the changes in load demand a feedback loop i.e PI controller is used. This feedback loop from the load is taken and given to the secondary input that is to the AC supply, so that whenever the load demand is not satisfied by solar then the AC supply will be added up to the solar supply to meet the load demand.

3. CIRCUIT DIAGRAM

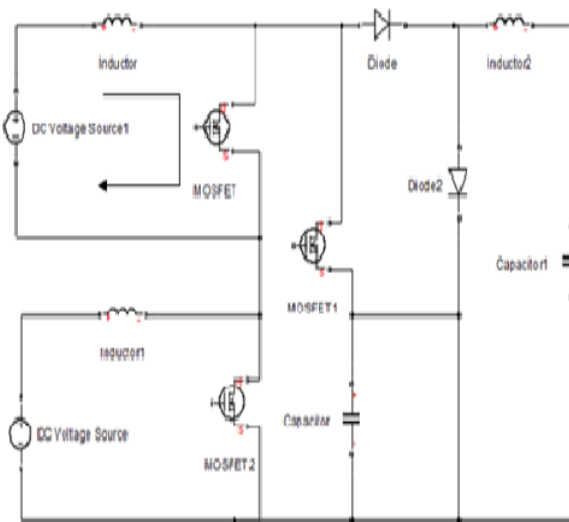


Figure 2- Equivalent Circuit of High Efficiency DC-DC Converter with Dual Input Power Sources

4. SINGLE MODE POWER SUPPLY

In this mode only one switch will be turned ON/OFF at a time to meet the load demand. The duty cycle for one switch will be

50% so that in the given 25kHz frequency 50% will be the on time & remaining off time.

Mode 1 [t0 –t1]: At t0 , the auxiliary inductor current iLa returned to zero. The switch S1 is continuously conducted and the auxiliary switch $Sais$ still turned OFF. The primary inductor $L1$ is linearly charged by the primary input voltage $V1$. The auxiliary switch voltage $vSais$ equal to the auxiliary capacitor voltage Va .

Mode 2 [t1 –t2]: At t1 , the switch S1 is turned OFF, the switch voltage $vS1$ is rising to the auxiliary capacitor voltage Va , and the auxiliary switch voltage $vSais$ decreasing to zero. The body diode of the auxiliary switch $Sais$ is conducted for receiving the primary inductor current $iL1$ to charge the auxiliary capacitor. Therefore, the switch current iSa is negative. Besides, the auxiliary inductor current linearly increases, and its slope is dependent on the auxiliary inductor voltage vLa , which is equal to $Va - Vo$. Continuously, the primary auxiliary diode $Da1$ is conducted.

Mode 3 [t2 –t3]: At t2 , the auxiliary switch Sa is turned ON with ZVS because the body diode has been already conducted for carrying the primary inductor current $iL1$. After the auxiliary inductor current iLa increases to be larger than the primary inductor current $iL1$, the auxiliary switch current iSa becomes positive. The discharging current from the auxiliary capacitor together with the primary inductor current $iL1$ releases the stored energy to the output voltage Vo .

Mode 4 [t3 –t4]: At t3 , the auxiliary switch Sa is turned OFF. Because the auxiliary inductor current iLa is greater than the primary inductor current $iL1$, the parasitic capacitor of the auxiliary switch Sa is charged by the auxiliary inductor current $iLaso$ that the auxiliary switch voltage $vSais$ rises. At the same time, the energy stored in the parasitic capacitor of the switch S1 will release to the output voltage Vo via the inductor current $iLaso$ that the switch voltage $vS1$ decreases.

The switch current $iSaf$ falls down to zero and the switch voltage $vSais$ rises to the auxiliary capacitor voltage Va . The body diode of the switch S1 is conducted for carrying the differential current without strain. Besides, the auxiliary inductor voltage $vLais$ is equal to $-Vo$, and the current $iLal$ linearly decreases. The energy stored in the auxiliary inductor La starts to discharge into the output voltage Vo as freewheeling.

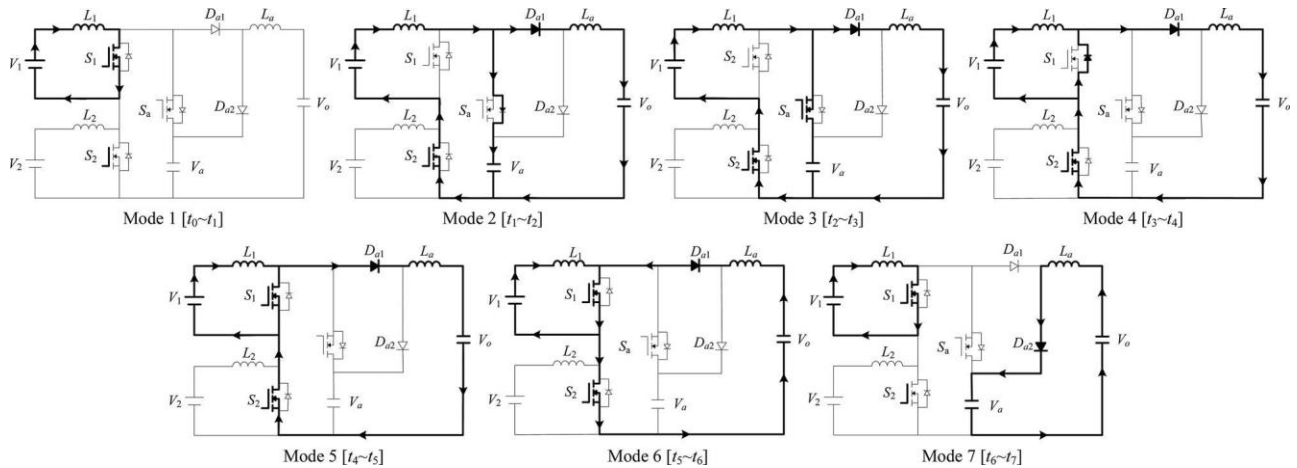


Fig.3.Topology modes in single power supply

Mode 5 [t4 –t5]: At t4 , the switch S1 is turned ON with ZVS upon the condition that the auxiliary inductor current $iLais$ still larger than the primary inductor current $iL1$. The auxiliary inductor current iLa continuously decreases with the slope $-Vo/La$. After the current $iLais$ smaller than the primary inductor current $iL1$, the switch current $iS1$ is positive.

Mode 6 [t5 –t6]: At t5 , the auxiliary inductor current $iLais$ equal to zero. In this mode, the parasitic capacitor of the primary auxiliary diode $Da1$ is charged by the output voltage Vo with a small reverse-recovery current.

Mode 7 [t6 –t7]: At t6 , the diode voltage $vDa1$ is rising to the output voltage Vo , the secondary auxiliary diode $Da2$ is conducted for receiving the auxiliary inductor current $iLato$ charge the auxiliary capacitor voltage Va , and then the auxiliary inductor current iLa returns to zero. In the single power-supply state with the primary input power, the switch SP 2 is always turned OFF and the switch $S2$ is triggered all the while. It means that the switch $S2$ works as a synchronous rectifier for avoiding the current to flow through its body diode and reducing the power losses in modes 2–7.

5. DUAL MODE POWER SUPPLY

When the proposed converter is operated in the dual power supply state with two input power sources, it can be taken as a superposition process of the primary and secondary input circuits. In this state, the summation of duty cycles $d1$ and $d2$ should be greater than 1, i.e., each of duty cycles $d1$ and $d2$ is securely greater than 0.5. Moreover, the symbols $da1$ and $da2$ denote the first and the second duty cycles of the switch Sa , respectively. $ddcm1$ and $ddcm2$ present the first and the second

duty cycles of the freewheeling times of the auxiliary inductor. In this mode both the switch will be conducting that is switch $S1$ and $S2$ and at the same time the auxiliary switch Sa will be turned off, as the auxiliary inductor current will return to zero, where as the inductor current $l1$ and $l2$ increases or charged by the input voltages $v1$ and $v2$, the dual input voltage source will operate together and flows through the diode, as the auxiliary switch is switched off the current does not flow through the switch hence current across to it is zero.

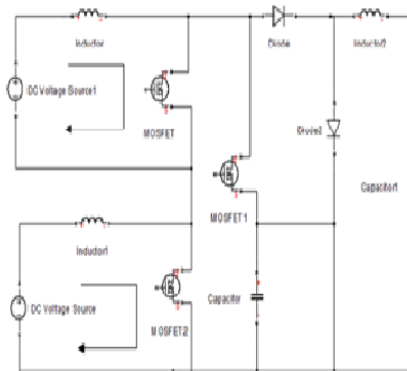


Fig-4. Equivalent Circuit of High Efficiency DC-DC Converter with Primary Input as Power Source

The proposed converter is operated in this dual power supply state with dual input power sources, it is considered as superposition of both the input source that is been conducting, only because of this mode of operation the efficiency of the system is increased as the output voltage obtained is more stable .This mode is only highlighted in this project, and the

entire concept used in this project is based on this dual power supply mode.

Mode 1 [t0 –t1]: At t0 , the auxiliary inductor current iL returned to zero. The switches S_1 and S_2 are continuously conducted. The auxiliary switch S_{ais} still turned OFF. The inductors L_1 and L_2 are linearly charged by the input voltages V_1 and V_2 , respectively.

Mode 2 [t1 –t2]: At t1 , the switch S_2 is turned OFF, the switch voltage vS_2 is rising to the auxiliary capacitor voltage V_a , and

the auxiliary switch voltage vS_{ais} decreasing to zero. The body diode of the auxiliary switch S_{ais} conducted for receiving the secondary inductor current iL_2 to charge the auxiliary capacitor. Therefore, the switch current iS_{ais} negative. Besides, the auxiliary inductor current iL_a linearly increases, and the slope is dependent on the auxiliary inductor voltage vL_a , which is equal to $V_a - V_o$. Continuously, the primary auxiliary diode D_{a1} is conducted.

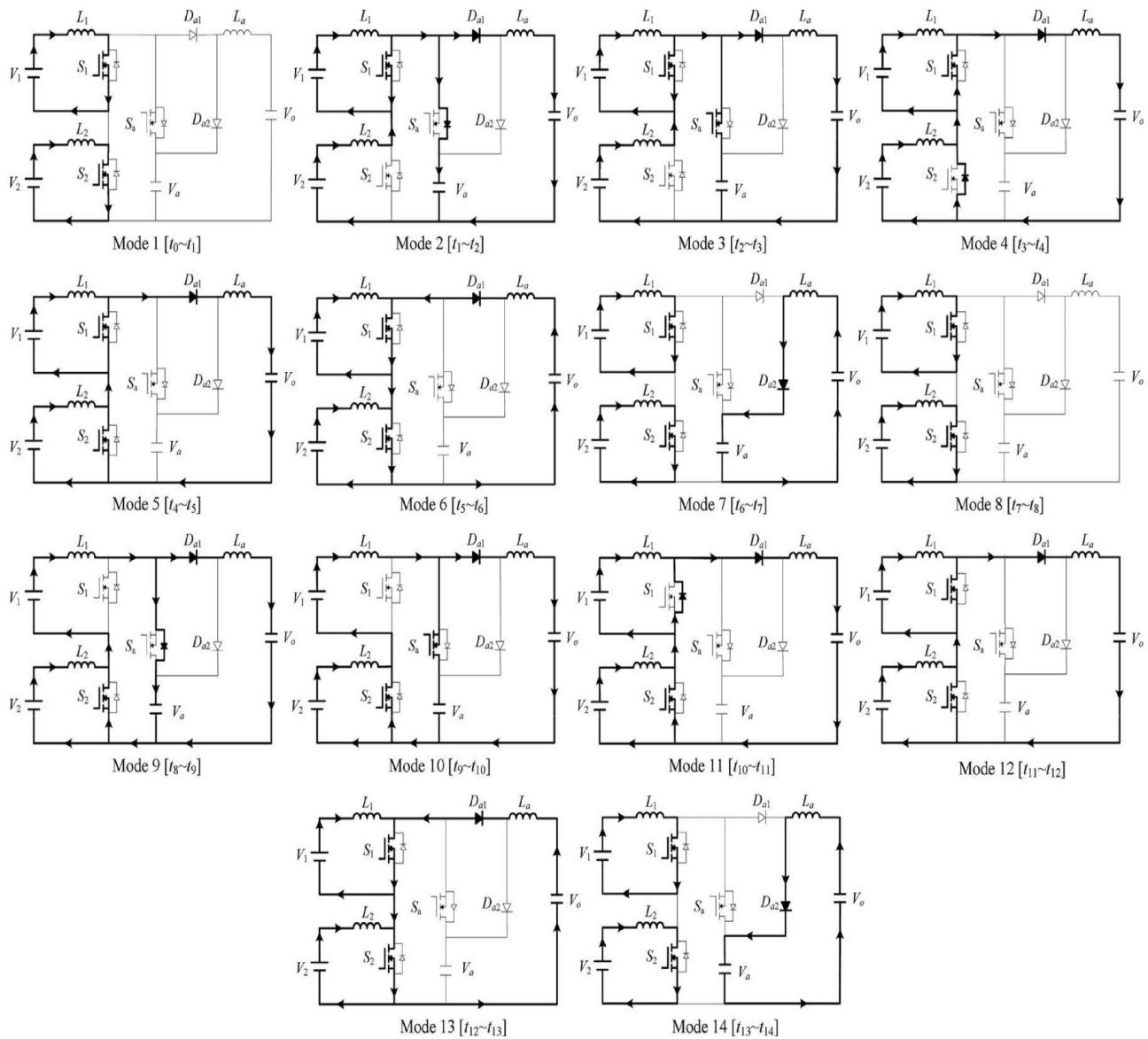


Fig-5. Topological modes in dual power-supply state.

Mode 3 [t2 –t3]: At t_2 , the auxiliary switch S_a is turned ON with ZVS. After the auxiliary inductor current i_{La} increases to be larger than the secondary inductor current i_{L2} , the auxiliary switch current i_{Sa} becomes positive. The discharging current from the auxiliary capacitor together with the secondary inductor current i_{L2} releases the stored energy to the output voltage V_o .

Mode 4 [t3 –t4]: At t_3 , the auxiliary switch S_a is turned OFF. Because the auxiliary inductor current i_{La} is greater than the secondary inductor current i_{L2} , the parasitic capacitor of the auxiliary switch S_a is charged by the auxiliary inductor current i_{La} , and the auxiliary switch voltage v_{Sa} rises. At the same time, the energy stored in the parasitic capacitor of the switch S_2 will release to the output voltage V_o via the inductor current i_{La} , and the switch voltage v_{S2} decreases.

Mode 5 [t4 –t5]: At t_5 , the switch S_2 is turned ON with ZVS upon the condition that the auxiliary inductor current i_{La} is still larger than the secondary inductor current i_{L2} . The auxiliary inductor current i_{La} continuously decreases with the slope $-V_o/L_a$. After the current i_{La} is smaller than the secondary inductor current i_{L2} , the switch current i_{S2} is positive. By the same way, the switch current i_{S1} becomes positive as well as i_{S2} .

Mode 6 [t5 –t6]: At t_5 , the auxiliary inductor current i_{La} is equal to zero. In this mode, the parasitic capacitor of the primary diode Da_1 is charged by the output voltage V_o with a small reverse-recovery current.

Mode 7 [t6 –t7]: At t_6 , the diode voltage v_{Da1} is rising to the output voltage V_o , the secondary auxiliary diode Da_2 is conducted for receiving the auxiliary inductor current i_{La} to charge the auxiliary capacitor.

Mode 8 [t7 –t8]: At t_7 , the auxiliary inductor current i_{La} returns to zero. The switches S_1 and S_2 are continuously conducted. Mode 8 is similar to mode 1.

Mode 9 [t8 –t9]: At t_8 , the switch S_1 is turned OFF, the switch voltage v_{S1} is rising to the auxiliary capacitor voltage V_a , and the auxiliary switch voltage v_{Sa} is decreasing to zero. The body diode of the auxiliary switch S_a is conducted for carrying the primary inductor current i_{L1} to charge the auxiliary capacitor. The auxiliary inductor current i_{La} linearly increases with the slope $(V_a - V_o)/L_a$. Continuously, the primary auxiliary diode Da_1 is conducted.

Mode 10 [t9 –t10]: At t_9 , the auxiliary switch S_a is turned ON with ZVS. After the auxiliary inductor current i_{La} increases to

be larger than the primary inductor current i_{L1} , the auxiliary switch current i_{Sa} becomes positive.

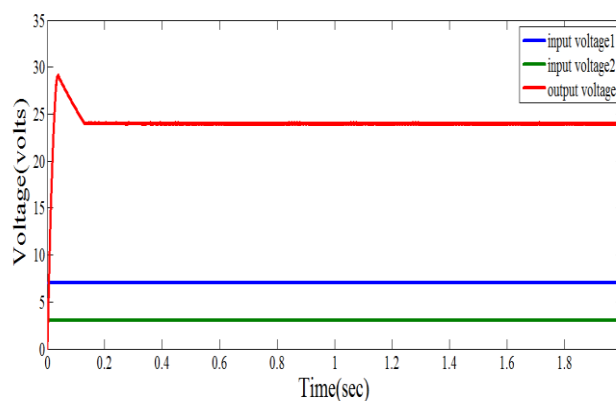
The discharging current from the auxiliary capacitor together with the primary inductor current i_{L1} releases the stored energy to the output voltage V_o .

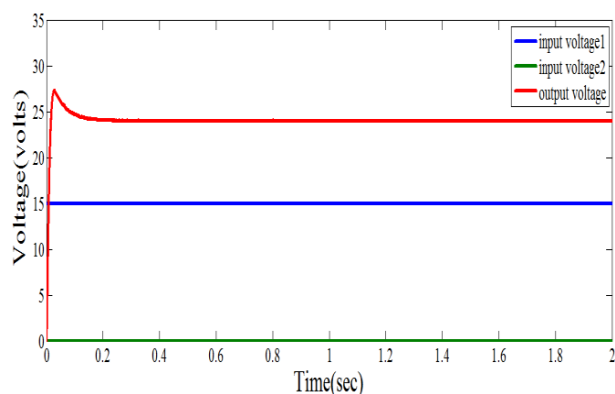
Mode 11 [t10–t11]: At t_{10} , the auxiliary switch S_a is turned OFF. Because the auxiliary inductor current i_{La} is greater than the primary inductor current i_{L1} , the parasitic capacitor of the auxiliary switch S_a is charged by the auxiliary inductor current i_{La} . At the same time, the energy stored in the parasitic capacitor of the switch S_1 will release to the output voltage V_o via the inductor current i_{La} . The switch current i_{S1} falls down to zero and the switch voltage v_{S1} rises to the auxiliary capacitor voltage V_a . Similar to mode 4, both the switches' currents i_{S1} and i_{S2} are negative. The energy stored in the auxiliary inductor L_a starts to discharge into the output voltage V_o as freewheeling.

Mode 12 [t11–t12]: At t_{11} , the switch S_1 is turned ON with ZVS. The auxiliary inductor current i_{La} continuously decreases with the slope $-V_o/L_a$. After the current i_{La} is smaller than the primary inductor current i_{L1} , the switch current i_{S1} is positive. By the same way, the switch current i_{S2} becomes positive as well as i_{S1} .

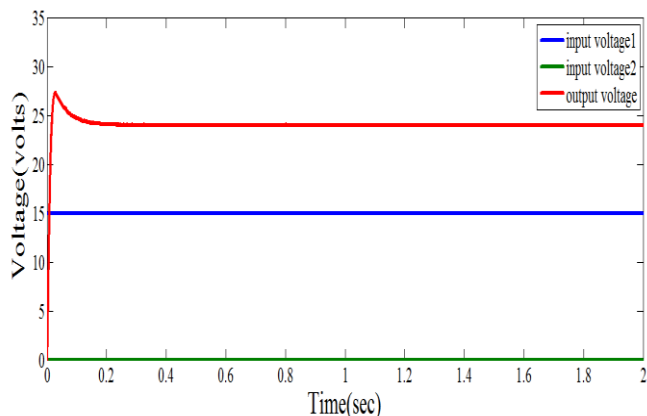
6. EXPERIMENTAL RESULTS

The proposed topology can be used to specific target applications for the high-voltage dc bus of an uninterruptible power supply or an inverter. The proposed converter can manipulate the high-efficiency power conversion with more than one input power source simultaneously to cope with the disadvantages of large size, complex topology, and expensive cost in conventional converter structure for individual power source.

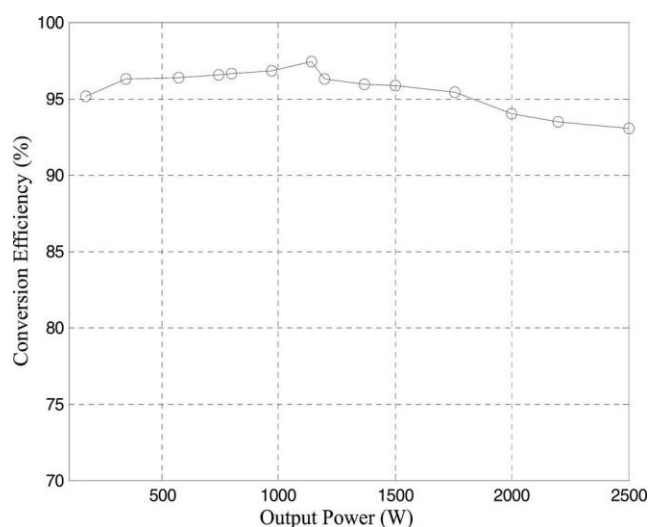




For an example of a hybrid PCS composed of two input power sources with an FC and a battery module, it has the following several merits: 1) it can manage the input power sources and improve system efficiency; 2) during the start of the system, the battery module powers the load to ensure that the FC cold starts easily; 3) when the load steps up, the battery module can provide the insufficient energy if the FC cannot respond quickly so that the dynamic characteristics of the entire system can be improved; and 4) the battery module can provide the FC can be decreased and the total cost of the whole system can be reduced.



In order to verify the effectiveness of the proposed ZVS dual-input converter, the corresponding experimental results are provided in this section. A power supply is used to emulate an FC taken as the primary power source with a maximum power of 2.5 kW, and the input voltage range is 120–170 V. Note that the summation of duty cycles d_1 and d_2 should be greater than 1 for regular operation in the dual power-supply state. Thus, each of duty cycles d_1 and d_2 should be bounded from a minimum value d_{min} to a maximum value d_{max} .



The minimum duty cycle d_{min} is designed to 0.55 slightly higher than a half of 1, and the maximum duty cycle d_{max} is designed to 0.83 for avoiding the lack of freewheeling time of the auxiliary inductor operating in DCM. According to the relation between input voltages and duty cycles in (31), the two input voltages should be in the same level. Therefore, the voltage range of another power supply is chosen as 120–170V for mimicking a battery module taken as the secondary power source with a maximum power of 2.5 kW. The proposed converter can boost the varied voltages of different power sources in the sense of hybrid power supply to a stable output dc voltage for the load demand.

7. CONCLUSION

A solar-AC hybrid generation system was proposed and implemented. This stand-alone hybrid generation system could effectively extract the maximum power from the solar energy sources. The proposed converter supplies continuous power to the load demand and greatly reduces the conduction and switching losses in the system. The simulation model of the proposed hybrid system is been developed using MATLAB/Simulink. Simulation results showed that the used PI controller could control the second switch properly so as to meet the load demand satisfactorily.

REFERENCES

- [1] M. Mahdavi and H. Farzanehfard, "Bridgeless SEPIC PFC Rectifier with Reduced Components and Conduction Losses," IEEE Transactions Industrial Electronics, vol. 58, No. 9, pp. 4153-4160, Sep. 2011.
- [2] Y. Jang and M. M. Jovanovic, "Bridgeless High-Power-Factor Buck Converter," IEEE Transactions Power Electron, vol. 26, No. 2, Feb. 2011.
- [3] M. ValanRajkumar, P.S. Manoharan, Modeling and Simulation of Three-phase DCMLI using SVPWM for Photovoltaic System, Springer Lecture Notes in Electrical Engineering, under the volume titled "Power Electronics & Renewable Energy Systems", Volume 326, Chapter No 5, January 2015, Pages 39-45.

- [4] M.ValanRajkumar, P.S.Manoharan, Harmonic Reduction of Fuzzy PI Controller based Three-Phase Seven-level DCMLI with SVPWM for Grid Connected Photovoltaic System, Journal International Review on Modeling and Simulations, Volume 6, No 3, June 2013, Pages 684-692.
- [5] A.Ravi, P.S.Manoharan, M.ValanRajkumar, "Harmonic Reduction of Three-Phase Multilevel Inverter for Grid connected Photovoltaic System using Closed Loop Switching Control", Journal-IREMOS, Volume 5, No 5, October 2012, Pages 1934-1942. ISSN: 1974-9821 (Print), 1974-982X (Online)
- [6] P.Thirumurugan, P.S.Manoharan, M.ValanRajkumar, "VLSI Based Inverter Switching Control" in the proceedings of International Conference on Mathematical Modeling and Applied Soft Computing MMASC'12 – Coimbatore Institute of Technology on July 2012, Vol-2 (Page):965-973.
- [7] C.Hemalatha, M.Valan Rajkumar, G.Vidhya Krishnan, "Simulation and Analysis for MPPT Control with Modified firefly algorithm for photovoltaic system", International Journal of Innovative Studies in Sciences and Engineering Technology, Volume 2, No 11, Nov.2016, Pages 48-52.
- [8] G.Vidhya Krishnan, M.Valan Rajkumar, C.Hemalatha, "Modeling and Simulation of 13-level Cascaded Hybrid Multilevel Inverter with less number of Switches", International Journal of Innovative Studies in Sciences and Engineering Technology, Volume 2, No 11, Nov.2016, Pages 43-47.
- [9] M.ValanRajkumar, P.S.Manoharan, FPGA Based Multilevel Cascaded Inverters with SVPWM Algorithm for Photovoltaic system, Elsevier Journal Solar Energy, Volume 87, Issue 1, January 2013, Pages 229-245.
- [10] B. Sanjay Gandhi, S. Sam Chelladurai, and Dr. D. Senthil Kumaran, "Process Optimization for Biodiesel Synthesis from Jatropha Curcas Oil", Taylor & Francis-Distributed Generation and Alternative Energy Journal, Vol.23, No.4, Page 6- 16, 2011.
- [11] B. Sanjay Gandhi and D. Senthil Kumaran, "The Production and Optimization of Biodiesel from Crude Jatropha Curcas Oil by a Two Step Process— An Indian Case Study Using Response Surface Methodology", Taylor & Francis-International Journal of Green Energy, Vol.113, No.10, Page 1084-1096, 2014.
- [12] M.ValanRajkumar, P.S.Manoharan, Space Vector Pulse Width Modulation of Three-Phase DCMLI with Neuro-Fuzzy MPPT for Photovoltaic System, World Journal of Modelling and Simulation, Volume 10, No 3, August 2014, Pages 193-205.
- [13] M.Valan Rajkumar, Prakasam, P. and Manoharan, P.S. (2016) Investigational Validation of PV Based DCDMLI Using Simplified SVM Algorithm Utilizing FPGA Tied with Independent Sources. Circuits and Systems, Volume 7, No 11, 3831-3848. <http://dx.doi.org/10.4236/cs.2016.711320>
- [14] R. Oruganti and M. Palaniapan, "Inductor Voltage Control of Buck Type Single-Phase AC-DC Converter," IEEE Transactions Power Electronics, vol. 15, No. 2, pp. 411-416, Mar. 2010.
- [15] M. A. Al-Saffar, E. H. Ismail, and A. J. Sabzali, "Integrated Buck Boost-Quadratic Buck PFC Rectifier for Universal Input Applications," IEEE Transactions Power Electronics, vol. 24, No. 12, pp. 2886-2896, Dec. 2009.
- [16] P.Thirumurugan, P.S.Manoharan, M.ValanRajkumar, VLSI Based Space Vector Pulse Width Modulation Switching Control in the proceedings of IEEE International Conference on Advanced Communication Control and Computing Technologies ICACCCT 2012 on August 2012, ISBN No. 978-1-4673-2045-0 (Print) (Page):366-370.
- [17] M.ValanRajkumar, P.S.Manoharan, "Modeling, Simulation and Harmonic Reduction of Three-Phase Multilevel Cascaded Inverters with SVPWM for Photovoltaic System", Journal International Review on Modeling and Simulations, Volume 6, No. 2, April 2013, Pages 342-350. ISSN: 1974-9821 (Print), 1974-982X (Online)
- [18] M.ValanRajkumar, P.S.Manoharan, "Modeling and Simulation of Five-level Five-phase Voltage Source Inverter for Photovoltaic Systems", Journal PrzegladElektrotechniczny, Volume 10, No. 10, October 2013, Pages 237-241. ISSN: 0033-2097 (Print)
- [19] T. Ching-Jung and C. Chern-Lin, "A Novel ZVT PWM Cuk Power Factor Corrector," IEEE Transactions Industrial Electronics, vol. 46, No. 4, pp. 780-787, Aug. 1999.
- [20] D. S. L. Simonetti, J. Sebastian, and J. Uceda, "The Discontinuous Conduction Mode Sepic and Cuk Power Factor Preregulators: Analysis and Design," IEEE Transactions Industrial Electronics, vol. 44, No. 5, pp. 630-637, Oct. 1997.
- [21] S. Chandrasekar and Gian Carlo Montanari, "Analysis of Partial Discharge Characteristics of Natural Esters as Dielectric Fluid for Electric Power Apparatus Applications," IEEE Transactions on Dielectrics and Electrical Insulation, Vol. 21, No. 3, pp.1251-1259, June 2014.
- [22] V.Jayaprakash Narayanan, B.Karthik and S.Chandrasekar," Flashover Prediction of Polymeric Insulators Using PD Signal Time-Frequency Analysis and BPA Neural Network Technique," Journal of Electrical Engineering and Technology. Vol. 9, Issue 4, pp. 1375-1384, 2014
- [23] P. F. de Melo, R. Gules, E. F. R. Romaneli, and R. C. Annunziato, "A Modified SEPIC Converter for High-Power-Factor Rectifier and Universal Input Voltage Applications," IEEE Transaction Power Electronics, vol. 25, No. 2, pp. 310-321, Feb. 2010.
- [24] R.Nagarajan and S.Sathishkumar, K.Balasubramani, C.Boobalan, S.Naveen, N.Sridhar. "Chopper Fed Speed Control of DC Motor Using PI Controller," IOSR- Journal of Electrical and Electronics Engineering (IOSR-JEEE), Vol.11 No.3, pp. 65-69, May-2016.
- [25] R.Nagarajan, S.Sathishkumar, S.Deepika, G.Keerthana, J.K.Kiruthika and R.Nandhini, "Implementation of Chopper Fed Speed Control of Separately Excited DC Motor Using PI Controller", International Journal of Engineering And Computer Science (IJECS), Volume 6, Issue 3, pp. 20629-20633, March 2017.
- [26] R.Nagarajan and M.Saravanan. "Performance Analysis of a Novel Reduced Switch Cascaded Multilevel Inverter," Journal of Power Electronics, Vol.14, No.1, pp. 48-60, Jan.2014.
- [27] C. Muniraj, K.Krishnamoorthi and S.Chandrasekar,"Investigation on Flashover Development Mechanism of Polymeric Insulators by Time Frequency Analysis", Journal of Electrical Engineering & Technology, Vol. 8, No. 6: 742-750, 2013.
- [28] P. Shanmugaraja, S. Vasanthi, D. Balamurugan, S. Chandrasekar, "Design and Implementation of Transport Relay Translator and its security Mitigations", International Journal of Engineering and Technology (IJET), Vol 5, No 4, pp3439-3442 Aug-Sep 2013.